Otology & Neurotology
32:163–170 © 2010, Otology & Neurotology, Inc.

Potential Role of Imatinib Mesylate (Gleevec, STI-571) in the Treatment of Vestibular Schwannoma

*Xabier Altuna, †Jay Patrick Lopez, †Michael Andrew Yu, ‡Maria Jesus Arandazi, †Jeffrey P. Harris, §Jessica Wang-Rodriguez, †Yi An, ‖Robert Dobrow, †Joni K. Doherty, and †Weg M. Ongkeko

**Servicio de Otorrinolaringología, Hospital Donosita, San Sebastian, Spain; †Division of Otolaryngology–Head and Neck Surgery, Department of Surgery, University of California, San Diego, California, U.S.A.; ‡Servicio de Anatomía Patológica, Hospital Donosita, San Sebastian, Spain; §Department of Pathology, University of California, San Diego, California; and ‖Department of Mathematics, Carleton College, Northfield, Minnesota, U.S.A.*

Hypothesis: To determine the expression of the tyrosine kinases platelet-derived growth factor receptor (PDGFR) and c-Kit in vestibular schwannoma (VS) and to determine the potential role of imatinib mesylate (Gleevec) in regulating the growth and cell death of this tumor.

Background: Protein tyrosine kinases are transmembrane tyrosine kinase receptors that transduce signals from inside and outside the cell and function as relay points for signaling pathways. They have a key role in numerous processes that affect cell proliferation, tumorigenesis, cancer invasion, metastasis, and modulation of apoptosis. A few of these kinases have been demonstrated to be overexpressed and dysregulated in many carcinomas, sarcomas, and benign tumors.

Methods: Immunohistochemical staining was used to investigate the expression of PDGFR and c-Kit in archived acoustic neuroma tissue. Clinical data including size of tumors, age, sex, and symptoms were correlated with kinase expression, whereas Western blot analysis and immunofluorescence were performed to demonstrate the expression and localization of PDGFR and c-Kit in HEI193, an immortalized VS cell line. Clonogenic survival assays were performed to assess proliferation inhibition by Gleevec. Gleevec's effect on the cell cycle profile also was investigated via flow cytometry analysis.

Results: Expression of PDGFR in the formalin-fixed VS tumor tissue was observed in 23 (67.5%) of the 34 samples. C-kit was expressed in 18 (52.9%) of the 34 samples. Western blot analysis demonstrates positive expression of c-Kit and PDGFR-Q in HEI193 and a primary VS culture. Western blot analysis showed downregulation of phospho-c-kit and phospho-PDGFR-Q with 5 and 10 uM Gleevec. Immunofluorescent staining of this cell line also reveals that PDGFR-β is localized primarily in the cytoplasm, whereas c-Kit is both nuclear and cytoplasmic. Cell cycle analysis of HEI193 96 hours after incubation with Gleevec indicates a dose-dependent increase in G1 from 61.6% to 70.7% and 74% at 5 and 10 uM of Gleevec, respectively. Colony formation assays demonstrate dose-dependent growth inhibition by Gleevec, in the HEI193 cell line as well as in a VS cell culture derived from a fresh tumor.

Conclusion: The expression of PDGFR-Q and c-Kit in VS tissue may indicate novel molecular targets involved in the development of this tumor. Direct inhibition of these molecules by Gleevec may have relevant therapeutic applications.

Key Words: Acoustic neuroma—c-kit—Gleevec—Imatinib mesylate—Platelet-derived growth factor receptor—STI-571—Tyrosine kinases—Vestibular schwannoma.
Otol Neurotol **32:**163–170, 2011.

Vestibular schwannomas (VSs) are rare, slow-growing neoplasms that originate from the VIIIth cranial nerve sheath. The vast majority of VSs develop from the Schwann cell investment of the vestibular portion of the vestibular cranial nerve. Currently, VSs are managed in 1 of 3 ways: 1) surgical excision of the tumor, 2) stereotactic radiation therapy, or 3) careful serial observation with magnetic resonance imaging (MRI). Improvements in surgical technique and postoperative care have enabled the safe removal of VSs. However, there remains a select group of individuals with VSs for whom nonoperative management would seem desirable, such as patients with significant cardiovascular or pulmonary disease, patients with minimal symptoms, or those with a VS in their only hearing ear (1). Furthermore, given the benign, slow-growing nature of this tumor and the gravity of the operation, the potential for a medical treatment of VS could revolutionize its management (2). Even if only a partial

Address correspondence and reprint requests to Weg M. Ongkeko, M.D., Ph.D., Division of Otolaryngology–Head and Neck Surgery, Department of Surgery, University of California, San Diego, La Jolla, CA 92093; E-mail: wegom@aol.com

X. A., J. P. L., and M. A. Y. contributed equally to this work.

The corresponding author had full access to all the data in the study and takes responsibility for the integrity of the data and the accuracy of the data analysis.

response could be achieved, avoidance of surgery in a select cohort would be a significant advancement.

The molecular biology in the development of VS is poorly understood. One category of patients who develop VSs are patients with neurofibromatosis 2 (NF2), an autosomal dominant disorder clinically characterized by bilateral VS and other intracranial and spinal tumors. The *NF2* gene, located in chromosome 22q (3), is a tumor suppressor gene that functions as a critical regulator of Schwann cell growth, with inactivation of the *NF2* gene being an essential step in tumorigenesis. The transcribed messenger RNA produces a protein designated as merlin or schwannomin (4,5).

Merlin loss occurs in both NF2 and sporadic VSs, the second category of VSs, which accounts for most VS tumors. Loss of chromosome 22q has been demonstrated in up to 45% of sporadic VS (6), and biallelic inactivation of the *NF2* gene has been demonstrated in almost all NF2-related VSs (7).

Aside from the *NF2*, there are several other genes implicated in the genesis of VS. The neuregulin gene family seems to act as schwann cell mitogens (8). These proteins signal via the c-erb receptor family, with c-erb 2 and 3 being the main receptors associated with schwann cells (9). Neuregulin-1/ErbB2 signaling has been implicated in the proliferation of VSs (10). Fibroblast growth factors and their receptors also are known to have a mitogenic effect on schwann cells (11).

Tumor expression of different cytokines and other factors that could regulate schwann cell proliferation and tumor growth have been addressed in studies of Ki-67 (4), proliferating cell nuclear antigen (12), nerve growth factor receptor (13), transforming growth factor receptor (14), fibroblast growth factor (14,15), vascular endothelial growth factor (16,17), epidermal growth factor receptor (2), and interleukin 6 (18).

In the last few years, there has been a tremendous interest in tyrosine kinases (TKs) as genes that may play a critical role in tumor development. Targeted therapy using small molecule inhibitors of these kinases has emerged as an attractive alternative to the toxic drugs used for chemotherapy. Clinical agents have been developed to inhibit several of these TKs, including EGFR, HER-2, Bcr-Abl, PDGFR, VEGF, and c-kit (19–21).

STI571 (imatinib mesylate, Gleevec; Novartis Pharmaceuticals Corporation, NJ, USA) is an example of such a small-molecule TK inhibitor. Gleevec, a drug designed to treat chronic myelogenous leukemia (CML) by inactivating the Bcr-Abl fusion kinase also directly interferes with TKs that are aberrantly activated in tumor cells. In solid tumors, Gleevec has been shown to inhibit the growth of ovarian cancer cells through platelet-derived growth factor receptor (PDGFR) inactivation (22). Gleevec also has been demonstrated to inhibit the growth of c-Kit–positive small cell lung cancer cell lines (23,24), PDGFR-expressing glioblastoma cells (25), and c-kit–positive gastrointestinal stromal tumor cell lines (26). These data suggest that Gleevec may be therapeutically relevant for other solid tumors in which activation of the c-Kit or PDGFR pathways may be responsible for tumorigenesis (27).

To determine if tyrosine kinases activation may have a role in the development of VS, we began by investigating the differential immunohistochemical expression profiles of the tyrosine kinases PDGFR and c-Kit in VSs. Clinical data including size of tumors, age, sex, and symptoms were correlated with kinase expression. To further investigate the role of tyrosine kinases, studies were performed using Gleevec on a virally (HPV E6/E7) immortalized human VS cell line, HEI193 (28). Because virally transformed cells may contain genetic modifications not normally present in VS cells, primary VS cells grown in culture also were used in our experiments for purposes of comparison.

MATERIALS AND METHODS

Tissue Samples

The records of all patients with a diagnosis of VS at the Servicio de Otorrinolaringología, Hospital Donostia, San Sebastián, Spain, between January 1991 and December 2002 were reviewed. Demographic data recorded on all patients included age, sex, and symptoms. Information on physical findings, such as audiogram results and tumor size; surgical approach; morbidities; and the last clinic visit also were all tabulated and evaluated.

Immunohistochemistry

The appropriate formalin-fixed, paraffin-embedded VSs were obtained from the archives of the Pathology department in accordance with the institutional review board of Hospital Donostia, San Sebastián, Spain. Approximately 4-μm sections were cut and placed on 3-aminopropyltriethoxysilane–coated slides. Immunohistochemical studies were performed using rabbit polyclonal antibodies against PDGFRβ and c-Kit (Santa Cruz Biotechnology, Santa Cruz, CA, USA). Negative control slides were from the same tissue but without the addition of the primary antibodies. Formalin-fixed, paraffin-embedded head and neck squamous cell carcinoma tissues were used as positive controls, and normal VIIIth cranial nerve was assessed for baseline c-kit and PDGFR-ß staining. The samples were heated for 1 hour at 60°C, deparaffinized in xylene and rehydrated in a graded series of ethanol. Antigen retrieval was performed by steam heating with Dako target retrieval solution. The endogenous peroxidase was quenched by 3% H_2O_2. Nonspecific binding of biotin and avidin was blocked by blocking solution (Protein Block Serum-Free; Dako, Carpinteria, CA, USA). The background staining was reduced with incubation with goat serum (1:20) for 60 minutes. Primary antibodies were placed on slides (1:100) and incubated for 1 hour at room temperature. Secondary antibodies conjugated with streptavidin/HRP (LSAB2; Dako) were used. The slides were washed and the antibody complex visualized by 3,3′-diamino-benzidine (DAB; Dako). The nuclei were counterstained by Gill's II hematoxylin.

Cases were considered positive if the staining was at least 2+ in the 1+-4+ scale, with more than 10% of the tumor cells staining above that of the background and negative control. Slides were scored as positive or negative by the authors (X. A. and M. J. A.), one of whom is a board certified pathologist.

Cell Culture and Western Blot

The HEI193 cell line was a gift from Dr. Lim (House Ear Institute, Los Angeles, CA, USA). VS cells were obtained from

fresh VS tumor during planned surgical removal, after obtaining the necessary IRB (No. 07-0135). Cell lines were cultured in Dulbecco's modified Eagle's medium (DMEM), supplemented with 10% fetal bovine serum, 10,000 unit/ml penicillin G sodium, 10 mg/ml streptomycin sulfate (Invitrogen Co.), and L-glutamine (Invitrogen Co., Carlsbad, CA, USA) at 37°C in 5% CO_2.

To determine the effect of Gleevec on HEI193, cells were treated with different concentrations of Gleevec for 24 hours, harvested, and evaluated by Western blot analysis. Cells were lysed with extraction buffer (1% [v/v] Triton X-100, 10 mmol/L Tris-HCl [pH, 7.4], 5 mmol/L ethylenediamine tetra-acetic acid, 50 mmol/L NaCl, 50 mmol/L NaF, 20 μg/mL aprotinin, 1 mmol/L phenylmethylsulfonyl fluoride, and 2 mmol/L Na_3VO_4) and subjected to 3 freeze/thaw cycles. The lysate was cleared by centrifugation at 20,000 × *g* for 10 minutes, and the protein concentration was measured. A total protein concentration of 30 μg was loaded per lane. Proteins were transferred onto nitrocellulose membranes and probed with the following primary antibodies: anti–c-kit (1:800), anti-PDGFR-ß (1:800), anti-phospho-c-kit (1:300), and anti-phospho-PDGFR-ß (1:300) (Cell Signaling Technology, Beverly, MA, USA), followed by incubation with the appropriate secondary antibodies. Membranes were then visualized with an enhanced chemiluminescence detection system (Pierce, Rockford, IL, USA). To demonstrate standardized loading, the membranes were probed with polyclonal antibody against β-actin ([1:1000]; Sigma-Aldrich, St. Louis, MO, USA).

Primary vestibular cells also were cultured from fresh tissue samples. After surgical removal, fresh tissues were immersed in ice-cold DMEM supplemented with gentamicin sulfate (Invitrogen Co.). Tissue samples were minced into 1- to 2-mm^3 explants and allowed to digest in DMEM containing 10% fetal bovine serum and 400 U/mL collagenase for 8 to 12 hours at 37°C into single cells. The tissue and cells were then collected, centrifuged, resuspended, and cultured in a cocktail consisting of 60% DMEM, 40% MCDB-210 (Sigma), 1% fetal bovine serum, 10 ng/ml recombinant human EGF (R&D Systems, Minneapolis, MN, USA), and 10 ng/ml recombinant PDGFR-BB (R&D Systems).

For protein analysis of PDGFR-β and c-Kit in fresh VS, a 25-mg piece of tissue was harvested and placed in cold lysis buffer for digestion. The sample was homogenized, and the final tissue in lysis buffer concentration was 5 mg/ml. The lysate was then centrifuged at 12,000 rpm. The pellet was discarded, and only the supernatant was retained for analysis. Western blot analysis was performed using anti-c-Kit (1:800), anti-PDGFR-ß (1:800) (Cell Signaling Technologies, Beverly, MA, USA) with MAPK (ERK1/2) as loading control.

Immunofluorescence Staining

Cells were plated on glass cover slides until they reached desired confluency. Cells were then fixed with 4% paraformaldehyde for 10 minutes. After washing with phosphate-buffered saline (PBS), the fixed cells were permeabilized with 0.2% Triton X-100. Cells were then incubated in the indicated primary antibodies, anti-c-kit (1:100) and anti-PDGFR-ß (1:100), for 1 hour at room temperature or overnight at 4°C. Primary antibodies were removed, and cells were washed with PBS and incubated in Alexa Fluor FITC-conjugated goat anti-mouse or goat antirabbit secondary antibodies (Molecular Probes; Invitrogen Co.) for 1 hour at room temperature. Slides were counterstained with 4',6'-diamidino-2-phenylindole dihydrochloride (DAPI) (1.0 ng/mL) for 1 hour before final embedding. Fluorescent images were obtained using Leica DMIRE2 inverted fluorescence microscope. Computer program Simple PCI was used for image capture.

Cell Cycle Distribution

To determine the cell cycle distribution and levels of Gleevec-induced cell death, 1×10^6 cells were harvested after the designated treatment and fixed in 50% cold ethanol overnight. The cells were then washed once with PBS and resuspended in a solution of PBS plus 0.1% Triton-X100, 2 mg/ml DNAase free RNaseA, and 0.02 mg/ml propidium iodide. Cells were analyzed by flow cytometry on a FACScan flow cytometer. Multicycle AV Cell Cycle software was used to calculate the fraction of cells in each phase of the cell cycle. Analyses were performed in triplicate, and indicated data represents the mean with standard deviation of the collected data.

Colony Formation Assay

Clonogenic survival assays were performed to assess the effectiveness of Gleevec in a VS cell line as well as in cells derived from a fresh VS tumor. The cells were plated in triplicate at 500 cells per 60 × 15 mm culture plate and grown in DMEM supplemented with 10% FBS, L-glutamine, and antibiotics. Twenty-four hours after plating, the cells were incubated with a range of doses of Gleevec (0, 0.1, 0.5, 1, 5, 10, 20, and 40 μM). Colonies were fixed and stained with a crystal violet/formalin solution and counted after 7 to 10 days using the AlphaImager 2200 and 1220 software (Alpha Innotech Co., San Leandro, CA, USA). Colonies are defined as having 50 cells or more.

TABLE 1. *Patient demographics and clinical data*

Case no.	Sex	Age (yr)	Side	Audiometry (0.5, −1, −2, and −3 kHz)	Approach
1	Male	25	L	Deafness[a]	Translabyrinthine
2	Male	68	L	40 dB	Translabyrinthine
3	Female	45	L	35 dB	Translabyrinthine
4	Female	63	L	Deafness	Translabyrinthine
5	Male	60	L	50 dB	Translabyrinthine
6	Female	28	L	Deafness	Translabyrinthine
7	Male	72	L	Deafness	Translabyrinthine
8	Male	60	R	Deafness	Translabyrinthine
9	Male	56	L	Deafness	Translabyrinthine
10	Female	60	L	Deafness	Translabyrinthine
11	Male	57	L	60 dB	Translabyrinthine
12	Female	45	R	Deafness	Middle Fosa
13	Female	64	L	50 dB	Translabyrinthine
14	Male	32	R	50 dB	Translabyrinthine
15	Male	59	L	Deafness	Translabyrinthine
16	Male	65	R	35 dB	Translabyrinthine
17	Male	29	L	20 dB	Translabyrinthine
18	Female	51	R	Normal	Middle Fosa
19	Male	64	L	Deafness	Translabyrinthine
20	Male	53	R	Deafness	Middle Fosa
21	Male	57	R	Deafness	Middle Fosa
22	Female	58	L	50 dB	Translabyrinthine
23	Female	28	L	Deafness	Retrosigmoid
24	Male	61	R	Not known	Retrosigmoid
25	Female	49	R	Not known	Retrosigmoid
26	Female	26	R	Deafness	Retrosigmoid
27	Female	25	L	Deafness	Retrosigmoid
28	Male	30	L	Deafness	Retrosigmoid
29	Male	48	L	Deafness	Translabyrinthine
30	Male	59	R	Deafness	Retrosigmoid
31	Female	63	L	60 dB	Retrosigmoid
32	Female	46	R	Not known	Retrosigmoid
33	Male	42	L	60 dB	Retrosigmoid
34	Female	34	R	50 dB	Translabyrinthine

[a]Deafness is defined as greater than 110 dB.

Statistics

For the association between the protein expression of c-Kit and PDGFR, the McNemar's test was used. For the association between age or tumor size with gene expression, the Student *t* test was used. The χ^2 test was used to evaluate the association between sex and gene expression. Finally, analysis of variance was used to calculate the statistical significance in the cell proliferation assays.

RESULTS

Demographics and Patient Profile

A total of 34 patients were studied (Table 1). The average age was 49.5 years (range, 25–72 yr), with a 19:15 male/female ratio. All of the cases were sporadic VSs; there were no NF2 patients in the cohort. Twenty tumors were on the left side, and 15 were on the right. There were no cases of bilateral VSs in this cohort. The most common presenting symptom was hearing loss, followed by tinnitus and disequilibrium. Four patients had hyposthesias in the trigeminal area, and 2 patients had facial nerve paralysis. Audiometric data (pure-tone averages were calculated as the average of the thresholds at 0.5, 1, 2, and 3 kHz) available on 30 of these 31 patients demonstrated asymmetric sensorineural hearing loss by pure tone, and 18 of these 30 had profound hearing loss. The remaining 12 had audiometry between 35 and 60 dB. The results in all 20 patients who underwent tone decay tests and stapedial reflexes indicated that the pathology of the disease was retrocochlear. Imaging evaluation by MRI was performed in all patients, whereas 12 patients had both computed tomography and MRI. The size of the tumors is represented in Table 2. Four patients underwent middle cranial fosa approach, 10 underwent retrosigmoid approach, and the remaining 20 underwent translabyrinthine approach.

TABLE 2. *PDGFR-ß and c-kit expression in acoustic neuroma*

Case no.	Maximum size (mm)	PDGFR-ß expression	c-Kit expression
1	15	Negative	Negative
2	10	Positive	Positive
3	25	Positive	Positive
4	12	Negative	Negative
5	10	Positive	Positive
6	30	Negative	Negative
7	10	Positive	Negative
8	20	Positive	Positive
9	15	Positive	Positive
10	12	Positive	Positive
11	40	Positive	Positive
12	3	Negative	Negative
13	25	Positive	Positive
14	8	Positive	Negative
15	20	Positive	Positive
16	8	Positive	Negative
17	15	Negative	Negative
18	8	Negative	Negative
19	10	Positive	Positive
20	7	Negative	Negative
21	8	Positive	Positive
22	15	Positive	Positive
23	30	Negative	Negative
24	Not known	Positive	Negative
25	Not known	Negative	Positive
26	40	Positive	Positive
27	32	Negative	Positive
28	25	Negative	Negative
29	10	Positive	Negative
30	35	Positive	Positive
31	8	Positive	Negative
32	Not known	Positive	Negative
33	15	Positive	Positive
34	10	Positive	Positive

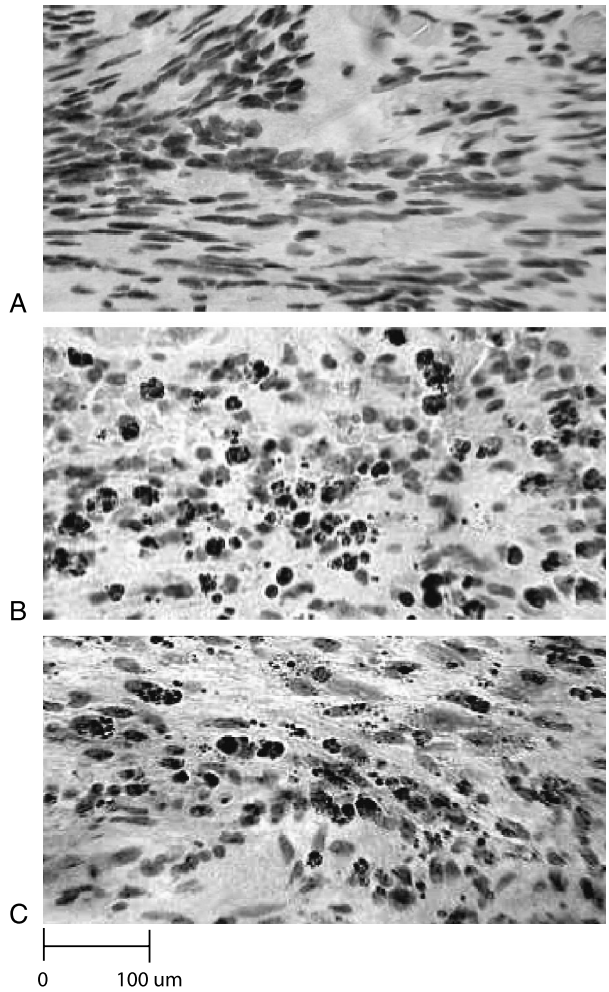

FIG. 1. Immunohistochemistry of VS tissue demonstrating (*A*) control, (*B*) c-Kit, and (*C*) PDGFR-β. Photographs were taken under 20× magnification.

Expression of the Tyrosine Kinases PDGFR and c-Kit in VS

Expression of PDGFR in the formalin-fixed tumor tissue was observed in 23 (67.5%) of the 34 samples. c-kit was expressed in 18 (52.9%) of the 34 samples (Table 2). Representative staining of PDGFR-β and c-Kit in vestibular schwannoma are shown (Fig. 1). All positive cases of PDGFR demonstrated cytoplasmic staining with membranous accentuation in the majority of the intensely staining cases. The average age among the PDGFR-positive

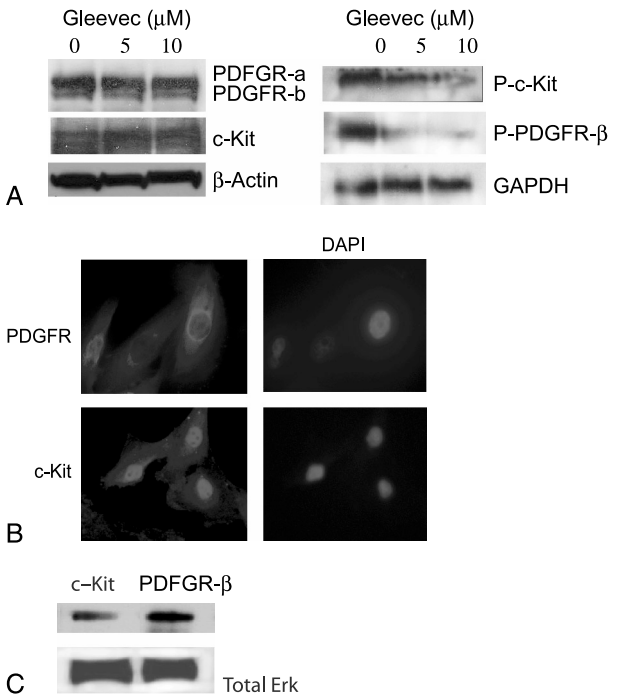

FIG. 2. Expression of the TKs PDGFR and c-Kit in HEI193. *A*, Western blot analysis showing protein expression of total c-Kit and PDGFR with different doses of Gleevec (left panel) and decrease in phosphorylated levels of c-Kit and PDGFR with increasing dose of Gleevec (right panel). *B*, Immunofluorescence demonstrating expression of the tyrosine kinases PDGFR primarily in the cytoplasm and c-Kit in both the nucleus and cytoplasm with intense staining in the nucleus. *C*, Western blot analysis demonstrating the presence of PDGFR-β and c-Kit in fresh VS tissue.

patients was 54.61 years, and that for the PDGFR-negative patients was 39.64 years ($p = 0.003$). For c-Kit expression, there was no significant difference in the age ($p = 0.18$), with an average of 52.94 years for positive patients and 49.19 for the negative ones. No difference in PDGFR positivity was related to tumor size. By contrast, c-Kit positive samples were bigger in size, with an average of 19.94 and 13.94 mm for c-Kit negative samples, although this difference was not statistically significant ($p = 0.07$). Coexpression of both PDGFR and c-Kit was observed in 16 (47.1%) of the 34 samples, and expression of PDGFR did not directly correlate with expression of c-Kit ($p = 0.5$). A study of the patients' sex and expression of the tyrosine kinase proteins revealed no correlation.

HEI193 and a Primary VS Culture Express c-Kit and PDGFR

Western blot analysis demonstrated that PDGFR and c-Kit are positively expressed in HEI193 cells and a primary VS cell culture (Fig. 2, A and C). Treatment of HEI193 cells with Gleevec has no effect on total protein levels of these tyrosine kinases (Fig. 2A). Furthermore, western analysis indicates that both 5 and 10 μM Gleevec can significantly downregulate levels of phospho-c-Kit and phospho-PDGFR-ß. Immunofluorescent staining reveals that PDGFR-ß is present and is localized primarily in the cytoplasm, whereas c-Kit is present in both the cytoplasm and nucleus, with intense expression in the nucleus (Fig. 2B).

Gleevec Causes a G_1 Accumulation in HEI193

Incubation of HEI193 cells with Gleevec causes very little change in cell cycle distribution in the first 48 hours (Fig. 3 and Table 3). At 96 hours of exposure to Gleevec, there is a dose-dependent increase in G_1 from 61.6% to 70.7% and 74% at 5 and 10 μM of Gleevec, respectively (Fig. 3 and Table 3). There also is a corresponding decrease of cells in S-phase from 26.6% to 17.7% and 13.2% with treatment with 5 and 10 μM of Gleevec, respectively. There is no significant change in the proportion of cells in G_2 in the presence or absence of Gleevec.

Gleevec Causes Inhibition of Cell Proliferation In HEI193 and Primary VS Cells

Colony formation assay was performed to assess the effect of Gleevec on long-term survival of HEI193 and

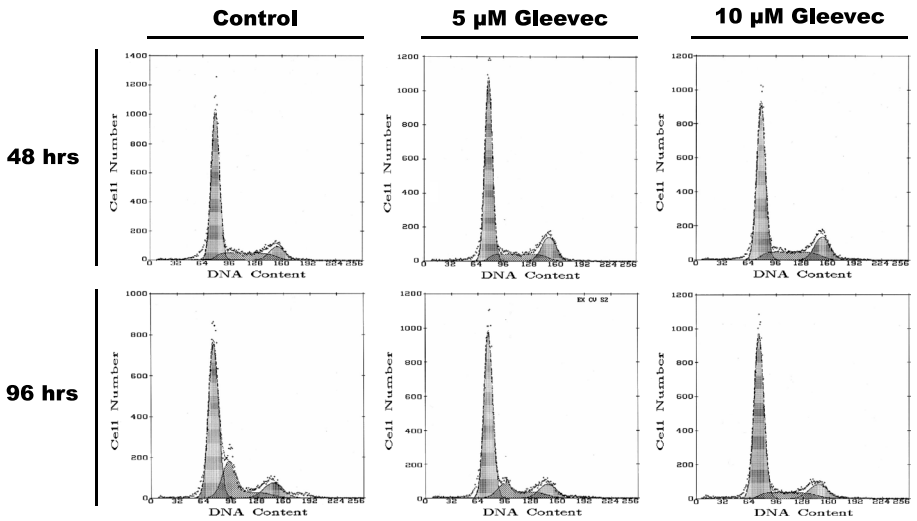

FIG. 3. Cell cycle distribution of HEI193 incubated with 0, 5, or 10 mM of Gleevec for 48 or 96 hours.

TABLE 3. *Cell cycle distribution of HEI193 cells in response to Gleevec*

Treatment	G_1 (%)	S (%)	G_2 (%)
Control—48 h	68.0	19.9	12.0
5 μM Gleevec—48 h	67.2	15.9	16.9
10 μM Gleevec—48 h	64.0	18.7	17.3
Control—96 h	61.6	26.6	11.7
5 μM Gleevec—96 h	70.7	17.7	11.5
10 μM Gleevec—96 h	74.0	13.2	12.8

primary VS cells. Figure 4 shows a dose-dependent decrease in the colony number of HEI193 cells (Fig. 4A) and a primary VS cell culture derived from a patient with sporadic VS (Fig. 4B) with increasing concentration of Gleevec with an IC50 of approximately 7 μM for both cell cultures. Complete inhibition of colony formation was approached at the dose of 40 μM. Cell doubling time was roughly 24 hours. The mean ± standard deviation of 3 separate repeated experiments is shown. Analysis of variance for both the HEI193 and the primary VS cell culture gives a $p < 0.01$.

DISCUSSION

The treatment for VS has improved significantly for the past several decades, resulting in lower mortality rates and reduced morbidity. Yet, even for a slow-growing tumor, surgical treatment still carries significant morbidity not only in terms of facial nerve paralysis or loss of hearing but also in postoperative headache that could severely affect the quality of life. Aside from this, in a subpopulation of patients who develop VS, surgery may not be an option, and therefore, alternative treatments are necessary. Furthermore, for recurrent VS or one in which a total excision is not feasible, medical therapy on its own or as an adjunct to surgery may have a role in managing this disease. Understanding the molecular biology of this

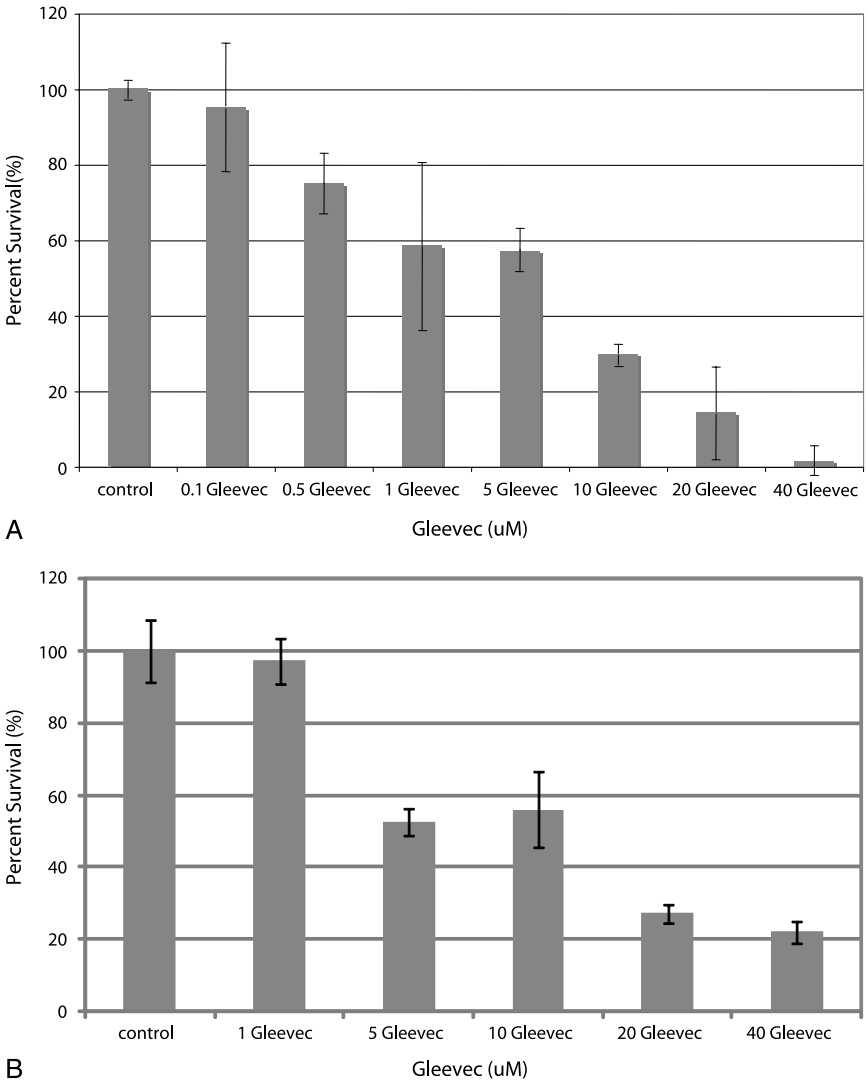

FIG. 4. Colony formation assay of (*A*) HEI193 and (*B*) primary VS cells derived from a sporadic VS with Gleevec.

disease is of critical importance for designing much needed alternative treatments.

In this study, we have demonstrated that the tyrosine kinases c-Kit and PDGFR-ß that have been implicated in tumor development are expressed at high levels in a significant proportion of VS. To our knowledge, this is the first time that the expression of both these tyrosine kinases has been investigated in VS. c-Kit protein is a receptor type TK, structurally related to PDGFR. It plays an important role in the development of hematopoietic cells, melanocytes, and germ cells. It has been described to be expressed in several human solid tumors including small cell lung cancer, gastrointestinal stromal cell tumors, germ cell tumors, breast cancer, salivary gland tumors, and head and neck squamous cell carcinoma (29–33). High levels of c-Kit have been reported in human schwann cells from patients with NF-1 (34). c-Kit also has been implicated as one of the components leading to the neurofibrosarcoma-derived Schwann cell hyperplasia observed in NF1 (35).

Aberrant expression of PDGFR has been linked to various human tumors including small cell lung carcinoma (36) and ovarian carcinoma (37). Constitutively active PDGFR tyrosine kinase is a common feature in idiopathic hypereosinophilic syndrome, eosinophilia-associated chronic myeloid disorder, chronic myelomonocytic leukemia, systemic mast cell disease, atypical chronic myelogenous leukemia, and dermatofibrosarcoma protuberans (38). The PDGFR family consists of the PDGFRα and β receptors that are stimulated by PDGF ligands. Both these receptors are known to be implicated in proliferation, intracellular organization, chemotaxis, apoptosis, and oncogenic transformation (38). Gleevec has been shown to have remarkable activity in these hematologic malignancies and solid tumors, presumably, through its action on PDGFR.

As both PDGFR-ß and c-Kit are expressed at high levels in a significant proportion of the VS samples surveyed, we then proceeded to determine if Gleevec, a known inhibitor of these kinases, could inhibit phosphorylation of these 2 target proteins. Western blot analysis confirmed that Gleevec can downregulate phosphorylation of both PDGFR-ß and c-Kit in HEI-193 at clinically relevant doses. We then sought to determine whether Gleevec would have an effect on the proliferation of VS. Using an immortalized human VS cell line, HEI193, and a VS cell culture, both of which express PDGFR-ß and c-Kit, we demonstrate that Gleevec can inhibit their proliferation in a dose-dependent manner. Furthermore, we demonstrate that Gleevec can alter the cell cycle distribution and induce cell death in HEI193 cells. These experiments suggest that tyrosine kinases may have a role in the proliferation of VS cells and imply the potential for the use of small molecule tyrosine kinase inhibitors. Receptor and nonreceptor tyrosine kinases (TKs) have recently been the focus of a lot of attention as they have emerged as clinically useful drug targets for certain neoplasms. The small molecule inhibitors developed for these kinases have very specific targets and, thus, are not only very effective but also have minimal side effects and may be ideal for combined therapies. It also is important to note that Gleevec is a fairly nonspecific TK inhibitor and may act against other kinase targets in VS aside from PDGR and c-Kit. Future studies should investigate whether Gleevec's ability to reduce cell growth also may be due to its interaction with other TKs implicated in Schwann cell neoplasia. As we learn more about the molecular biology of VS, even more specific and effective TK inhibitors can be developed that could revolutionize the treatment of this disease.

REFERENCES

1. Strasnick B, Glasscock ME 3rd, Haynes D, et al. The natural history of untreated acoustic neuromas. *Laryngoscope* 1994;104:1115–9.
2. Sturgis EM, Woll SS, Aydin F, et al. Epidermal growth factor receptor expression by acoustic neuromas. *Laryngoscope* 1996;106: 457–62.
3. Zang KD. Cytological and cytogenetical studies on human meningioma. *Cancer Genet Cytogenet* 1982;6:249–74.
4. Trofatter JA, MacCollin MM, Rutter JL, et al. A novel moesin-, ezrin-, radixin-like gene is a candidate for the neurofibromatosis 2 tumor suppressor. *Cell* 1993;72:791–800.
5. Rouleau GA, Merel P, Lutchman M, et al. Alteration in a new gene encoding a putative membrane-organizing protein causes neurofibromatosis type 2. *Nature* 1993;363:515–21.
6. Seizinger BR, Martuza RL, Gusella JF. Loss of genes on chromosome 22 in tumorigenesis of human acoustic neuroma. *Nature* 1986;322:644–7.
7. Jacoby LB, MacCollin M, Barone R, et al. Frequency and distribution of NF2 mutations in schwannomas. *Genes Chromosomes Cancer* 1996;17:45–55.
8. Morrissey TK, Levi AD, Nuijens A, et al. Axon-induced mitogenesis of human Schwann cells involves heregulin and p185erbB2. *Proc Natl Acad Sci U S A* 1995;92:1431–5.
9. Carroll SL, Miller ML, Frohnert PW, et al. Expression of neuregulins and their putative receptors, ErbB2 and ErbB3, is induced during Wallerian degeneration. *J Neurosci* 1997;17:1642–59.
10. Hansen MR, Roehm PC, Chatterjee P, et al. Constitutive neuregulin-1/ErbB signaling contributes to human vestibular schwannoma proliferation. *Glia* 2006;53:593–600.
11. Tzeng SF, Deibler GE, DeVries GH. Myelin basic protein and myelin basic protein peptides induce the proliferation of Schwann cells via ganglioside GM1 and the FGF receptor. *Neurochem Res* 1999;24:255–60.
12. Wiet RJ, Ruby SG, Bauer GP. Proliferating cell nuclear antigen in the determination of growth rates in acoustic neuromas. *Am J Otol* 1994;15:294–8.
13. Matsunaga T, Hosoda Y, Kanzaki J. Ultrastructural localization of nerve growth factor receptor in acoustic neurinoma. *Acta Otolaryngol Suppl* 1991;487:69–74.
14. Cardillo MR, Filipo R, Monini S, et al. Transforming growth factor-beta1 expression in human acoustic neuroma. *Am J Otol* 1999;20: 65–8.
15. O'Reilly BF, Kishore A, Crowther JA, et al. Correlation of growth factor receptor expression with clinical growth in vestibular schwannomas. *Otol Neurotol* 2004;25:791–6.
16. Caye-Thomasen P, Baandrup L, Jacobsen GK, et al. Immunohistochemical demonstration of vascular endothelial growth factor in vestibular schwannomas correlates to tumor growth rate. *Laryngoscope* 2003;113:2129–34.
17. Brieger J, Bedavanija A, Lehr HA, et al. Expression of angiogenic growth factors in acoustic neurinoma. *Acta Otolaryngol* 2003;123: 1040–5.
18. Adams EF, Rafferty B, Mower J, et al. Human acoustic neuromas secrete interleukin-6 in cell culture: possible autocrine regulation of cell proliferation. *Neurosurgery* 1994;35:434–8; discussion 8.
19. Vlahovic G, Crawford J. Activation of tyrosine kinases in cancer. *Oncologist* 2003;8:531–8.

20. Blume-Jensen P, Hunter T. Oncogenic kinase signalling. *Nature* 2001;411:355–65.
21. Levitzki A, Gazit A. Tyrosine kinase inhibition: an approach to drug development. *Science* 1995;267:1782–8.
22. Matei D, Chang DD, Jeng MH. Imatinib mesylate (Gleevec) inhibits ovarian cancer cell growth through a mechanism dependent on platelet-derived growth factor receptor alpha and Akt inactivation. *Clin Cancer Res* 2004;10:681–90.
23. Wang WL, Healy ME, Sattler M, et al. Growth inhibition and modulation of kinase pathways of small cell lung cancer cell lines by the novel tyrosine kinase inhibitor STI 571. *Oncogene* 2000; 19:3521–8.
24. Krystal GW, Honsawek S, Litz J, et al. The selective tyrosine kinase inhibitor STI571 inhibits small cell lung cancer growth. *Clin Cancer Res* 2000;6:3319–26.
25. Kilic T, Alberta JA, Zdunek PR, et al. Intracranial inhibition of platelet-derived growth factor-mediated glioblastoma cell growth by an orally active kinase inhibitor of the 2-phenylaminopyrimidine class. *Cancer Res* 2000;60:5143–50.
26. Tuveson DA, Willis NA, Jacks T, et al. STI571 inactivation of the gastrointestinal stromal tumor c-KIT oncoprotein: biological and clinical implications. *Oncogene* 2001;20:5054–8.
27. George D. Platelet-derived growth factor receptors: a therapeutic target in solid tumors. *Semin Oncol* 2001;28:27–33.
28. Hung G, Li X, Faudoa R, et al. Establishment and characterization of a schwannoma cell line from a patient with neurofibromatosis 2. *Int J Oncol* 2002;20:475–82.
29. Strohmeyer T, Peter S, Hartmann M, et al. Expression of the hst-1 and c-kit protooncogenes in human testicular germ cell tumors. *Cancer Res* 1991;51:1811–6.
30. Ishikawa K, Komuro T, Hirota S, et al. Ultrastructural identification of the c-kit-expressing interstitial cells in the rat stomach: a comparison of control and Ws/Ws mutant rats. *Cell Tissue Res* 1997;289:137–43.
31. Jeng YM, Lin CY, Hsu HC. Expression of the c-kit protein is associated with certain subtypes of salivary gland carcinoma. *Cancer Lett* 2000;154:107–11.
32. Ongkeko WM, Altuna X, Weisman RA, et al. Expression of protein tyrosine kinases in head and neck squamous cell carcinomas. *Am J Clin Pathol* 2005;124:71–6.
33. Sekido Y, Obata Y, Ueda R, et al. Preferential expression of c-kit protooncogene transcripts in small cell lung cancer. *Cancer Res* 1991;51:2416–9.
34. Ryan JJ, Klein KA, Neuberger TJ, et al. Role for the stem cell factor/KIT complex in Schwann cell neoplasia and mast cell proliferation associated with neurofibromatosis. *J Neurosci Res* 1994; 37:415–32.
35. Badache A, Muja N, De Vries GH. Expression of Kit in neurofibromin-deficient human Schwann cells: role in Schwann cell hyperplasia associated with type 1 neurofibromatosis. *Oncogene* 1998;17:795–800.
36. Kawai T, Hiroi S, Torikata C. Expression in lung carcinomas of platelet-derived growth factor and its receptors. *Lab Invest* 1997; 77:431–6.
37. Henriksen R, Funa K, Wilander E, et al. Expression and prognostic significance of platelet-derived growth factor and its receptors in epithelial ovarian neoplasms. *Cancer Res* 1993;53:4550–4.
38. Tibes R, Trent J, Kurzrock R. Tyrosine kinase inhibitors and the dawn of molecular cancer therapeutics. *Annu Rev Pharmacol Toxicol* 2005;45:357–84.